Spatial ordering of islands grown on patterned surfaces

Choongseop Lee and Albert-László Barabási
Department of Physics, University of Notre Dame, Notre Dame, Indiana 46556

(Received 13 July 1998; accepted for publication 3 September 1998)

We demonstrate that growth on a sample patterned with an ordered defect array can lead to islands with rather narrow size distribution. However, improvement in the size distribution is achieved only if the growth conditions (flux and temperature) have optimal values, determined by the patterning length scale. Since the scanning tunelling and the atomic force microscopes are capable of inducing surface perturbations that act as potential preferential nucleation sites, our work demonstrates that nanoscale surface patterning can improve the ordering of platelets and self-assembled quantum dots.
 [S0003-6951(98)03444-5]

Heteroepitaxial growth of highly strained islands has gained interest lately as it offers the possibility to fabricate islands with very narrow size distribution. Thanks to their small size, these islands are candidates for one dimensional electron confinement. Two different island types have been found to have interesting optical properties. First, it has been recently demonstrated that InAs *submonolayer islands*, often called *platelets*, grown on and capped with GaAs, lead to dramatic increase of the exciton oscillator strength over excitons in the bulk material, and have narrow luminescence linewidth.[1] Second, for larger coverages highly strained three dimensional islands form, coined self-assembled quantum dots (SAQDs),[2] that hold potential for numerous device applications, from lasers to diodes and detectors. However, to turn the self-assembling process into actual devices we need to reach unprecedented control over the island characteristics, that include *small* (ideally close to zero) *size distribution, tunable island sizes, and large island density.*

One way to achieve these goals is to obtain precise control over the position of the islands, since one expects that spatial ordering would translate into narrower size distribution as well.[3] Consequently, different methods that have the potential to lead to spatially ordered SAQDs, such as growth on patterned surfaces,[4] aligning along misfit dislocations[5] or along surface steps,[6] are subject of much interest lately.

However, to reach the controlled positioning of the islands, we need to use patterning that offers nanoscale precision in the first place. Recently it has been demonstrated that the scanning tunelling microscope (STM) and the atomic force microscope (AFM) are capable of performing small surface perturbations on the surface by depositing individual atoms,[7] small clusters or generating mesas or holes.[8] These surface modifications (defects) can act as potential nucleation sites, and their position can be controlled with nanometer precision. Thus STM/AFM tips can be used to pattern the surface with a mesh of spatially ordered defects.[9] Growth on such patterned surface is expected to lead to preferential island formation around the defects. However, since the nucleation of islands at positions *different* from those determined by the pattern cannot be excluded, it is not clear that such patterning will improve the positioning and the size distribution of the islands.

In this letter we demonstrate that the combination of an ordered defect array with suitably chosen growth conditions for island formation has the potential to produce islands with properties that are superior to the currently grown samples. For this we calculate the effect of an impurity mesh on the island sizes and positions using atomistic Monte Carlo simulations. The simulations indicate that for a given pattern there exists an optimal set of growth conditions at which the error rate (the nucleation of an island at a position different from that determined by impurities) is the smallest and the most uniform islands form. We discuss the impact of these result on the growth of platelets and SAQDs.

The initial stages of island formation are determined by the nucleation of small precursor islands, often called platelets.[10,11] These two-dimensional (2D) islands are relatively small, strain effects are not yet relevant, thus their nucleation is governed by the laws of submonolayer epitaxy.[12,13] The phenomenology is quite well understood:[13,14] the atoms deposited on the surface diffuse until they meet another atom or the edge of an island, whereupon they stick. The diffusion probability depends on the energy $E=E_0+nE_N$, where E_N is the energy of the bond formed by the atom with its n nearest neighbors (so $n=0$, 1, 2, 3, and 4) and E_0 is the activation energy for monomer surface diffusion. Since the formation of the critical nucleus is a random event, the position of the 2D islands is random. If there are impurities or defects on the substrate, they can serve as nucleation sites. The precise interaction of the adatoms and the defects is determined by the nature of the defect. Here we will consider a simple model, in which the defects are impurity atoms. The difference between an impurity and an adatom comes in the activation energy for surface diffusion for the impurity, E_0^I, and the binding energy between the adatoms and the impurity atom, E_N^I. If E_0^I is *larger* than E_0, the impurity is less mobile, i.e., once it is deposited, it diffuses slower than the adatoms. Even a small $(E_0^I-E_0)$ difference can translate into an impurity diffusion so slow, that within the time scales defined by deposition ($\propto 1/F$, where F is the flux) the impurities are practically immobile. Finally, the condition that an impurity serves as a nucleation site (i.e., adatoms that attach to it do not diffuse away) is $E_N^I > E_N$.

In the simulations we assume that a regular mesh of impurity atoms forming a two-dimensional square lattice has been deposited on the substrate, such that the distance between the impurity atoms is ℓ_i. On this substrate we then deposit atoms with coverage θ.

Figure 1(a)–1(c) show the island morphologies for three

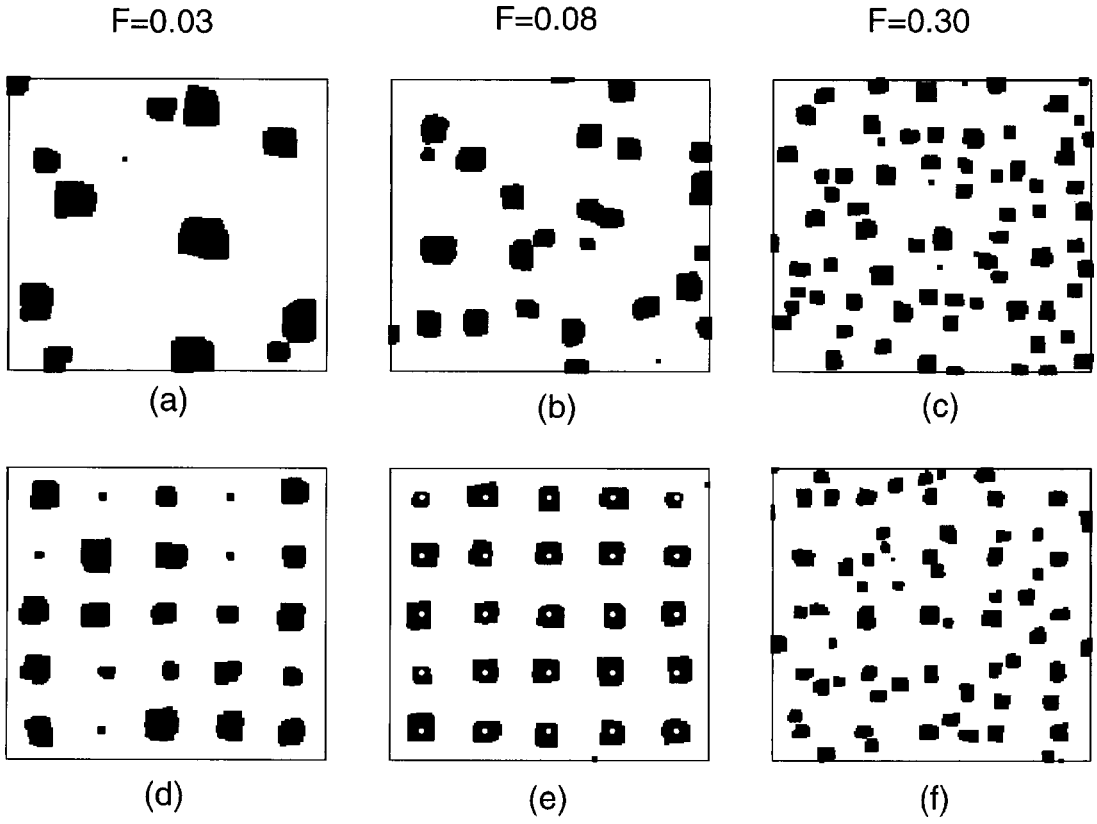

FIG. 1. Island morphologies obtained on an impurity free substrate (a)–(c) as well as on a surface patterned with impurities (d)–(f), each shown for coverage $\theta=0.1$, and for different deposition fluxes. The parameters in the simulations are system size $L=400$, $T=400$ K, $E_0=1.3$ eV, $E_N=0.3$ eV, $E_0^I=2.6$ eV, $E_N^I=0.6$ eV, and $\ell_i=40$. In (e) we show as small circles the position of the impurities that were used in (d)–(f).

different fluxes, grown on an impurity free substrate. In agreement with submonolayer epitaxy, as the flux increases, it leads to a decreasing average island size, $\langle s\rangle$, and an increasing island density, ρ. In contrast, as Fig. 1(d)–1(f) indicates, the impurities have a strong effect on both the size and the position of the islands. For small fluxes, when $l_d \gg \ell_i$, islands are nucleated only around the impurities [Fig. 1(d)]. However, in this regime the island sizes are not uniform, but we observe the *coexistence of small and large islands*. In contrast, for intermediate fluxes, when $l_d \simeq \ell_i$, all islands have approximately the *same size* [Fig. 1(e)]. Finally, for large fluxes, when $l_d \ll \ell_i$, islands are nucleated randomly, and while the impurities still serve as preferential nucleation sites, there are additional islands, and the observed configuration is indistinguishable from the impurity free case [Fig. 1(f)].

As Fig. 1 illustrates, for a given impurity mesh ℓ_i there is an optimal flux at which the islands nucleate only on impurities and their size is rather uniform [e.g., Fig. 1(e)]. This optimal flux can be measured by calculating the relative width of the island size distribution, w, defined as $w=\overline{w}/\langle s\rangle$ where $\overline{w}=\langle s^2\rangle-\langle s\rangle^2$ is the width of the size distribution, and $\langle ...\rangle$ denotes ensemble average. The smaller w is, the smaller the fluctuations are in the island sizes. In Fig. 2(a) we show w as a function of flux for the impurity free case (w_0) and for growth with impurities (w_I). For small fluxes the coexistence of the small and large islands makes w_I rather large, much larger than w_0. However, there is a window of fluxes for which w_I is smaller than w_0, corresponding to more uniform islands. In particular, there is an optimal flux, $F_{\rm opt}$, at which w_I has a minima (in contrast with the impurity free case, for which w_0 monotonously increases). In the following we discuss separately each of the three growth regimes, offering quantitative support for the qualitative conclusions derived from Fig. 1.

Regime I; Small fluxes ($l_d \gg \ell_i$): In this regime, the impurities are the only nucleation sites. However, the typical separation between islands on the impurity free substrate is much larger than ℓ_i [see Fig. 1(a)]. As a consequence, only some impurities nucleate large islands, leading to the coexistence of distinctly small and large islands [Fig. 1(d)]. This observation is supported by the island size distribution, which is bimodal: we observe a rather narrow peak corresponding to small islands ($s\simeq 5-10$), and a wider peak corresponding to the larger islands ($s\simeq 100$). However, since islands are nucleated only by the impurities, the island density in this regime is constant, being equal to the impurity density, in contrast with the impurity free case for which ρ increases with F [see Fig. 2(b)]. Furthermore, in this regime the average island size, $\langle s\rangle$, is also independent of the flux [see Fig. 2(c)].

Regime II; Optimal flux ($l_d \simeq \ell_i$): The most striking result of our simulations is that there is an optimal flux, $F_{\rm opt}$, at which approximately equal sized islands are nucleated only on sites predetermined by the impurity mesh. The improvement in the island size distribution, compared to the impurity free case, can be visually observed in Fig. 1 and quantitatively supported by w, shown in Fig. 2(a). As Figs. 2(b) and 2(c) indicate, $F_{\rm opt}$ is the flux at which $\langle s\rangle$ and ρ for the impurity induced growth cross over to the impurity free

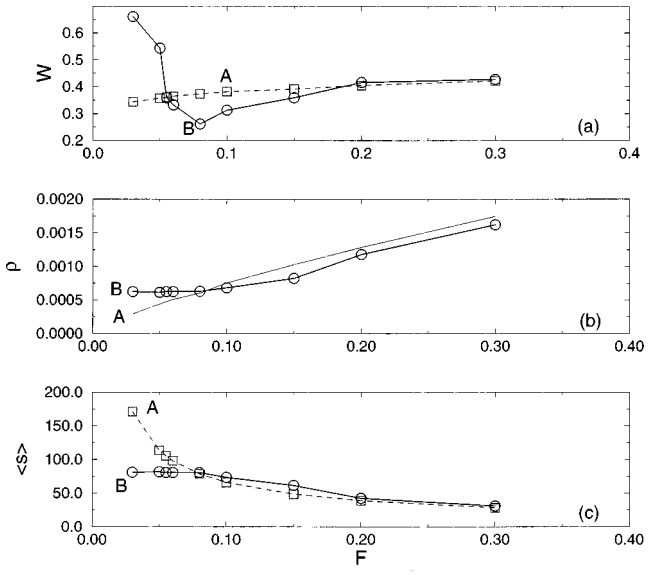

FIG. 2. (a) Relative width of the island size distribution for surfaces without (A) and with impurities (B) as a function of the flux F. w increases monotonously for the surface without impurities. (b) Island density vs flux for the surfaces without (A) and with impurities (B). The island density increasing with F for the surface without impurities (A). With impurities, for small fluxes the island density is constant, being equal to the impurity density. (c) Average island size vs flux for the surfaces without (A) and with impurities (B). The average island size decreases for the surface without impurities (A), following $\langle s\rangle \sim F^{-\psi_d}$. For the surfaces with impurities, however, the average island size is constant until $F \cong 0.08$, and then decreases for larger F, converging to the impurity free curve.

values. The optimal flux, F_{opt}, corresponds to the case when the *natural separation of the islands, l_d, is equal to the impurity separation* ℓ_i, thus the impurities do not nucleate new islands, nor suppress island nucleation, but affect only the position of the islands. And since the equally spaced islands collect adatoms from approximately the same area, their size is more uniform than that of randomly positioned islands grown on the impurity free substrate. Note that in general there are three different sources of randomness in the system: the randomness in the capture areas,[3] fluctuations in the density of deposited atoms, and in adatom diffusion, allowing the atoms to move away from the area to which they have been deposited. While the deposition and diffusion noise cannot be avoided, the capture areas of the islands can be modified by initiating the nucleation on a mesh.

Regime III; Large fluxes ($l_d \ll \ell_i$): In this regime the separation between the islands grown on the impurity free substrate is smaller than the lattice constant ℓ_i of the impurity mesh, thus islands nucleate on interstitial positions as well [Fig. 1(f)]. Consequently, there is no difference between the impurity induced and impurity free growth: the two systems have the same island density [Fig. 2(b)] and the same average island size [Fig. 2(c)]. Similarly, the relative width of the islands is the same as for the impurity free growth.

The presented simulations capture the early stages of island formation, when strain effects are not yet relevant. Strain is known to further decrease the size distribution of the islands: self-limiting mechanism, acting through biased surface diffusion and/or strain induced enhanced adatom detachment from large islands discourage the formation of large islands, and thus lead to narrower island size distribution.[11,12] Consequently, we expect that the beneficial results of the impurities will be further improved if strain is taken into consideration.

While our simulations included impurities as nucleation sites, we expect that the main results would apply if instead of impurity atoms small clusters are deposited, or the STM is used to create small mesas or holes on the surface, as long as these defects act as *preferential nucleation sites*. The recent development of parallel AFM tips, consisting of over a hundred individual tips, allow the parallel creation of ordered surface defects with a single touchdown, thus foreseeing the rather fast nanometer scale patterning of surfaces for device applications. Our main result is that the mere deposition of these nucleation centers is not enough for improvement in their island characteristics: improvements are obtained only for carefully tuned growth conditions so that the growth takes place at an optimal flux. Since it is rather easy to tune the flux in an molecular beam epitaxy (MBE) chamber, it is possible to locate this optimal flux experimentally.[15] Naturally, for each ℓ_i there will be a different F_{opt}, which has to be determined independently, but the very existence of such an optimal flux indicates that the controlled deposition of impurities has the potential to produce high quality samples with potentially superior optical characteristics.

This research was supported by the Office of Naval Research under Award No. N00014-98-1-0575.

[1] P. D. Wang, N. N. Ledentsov, C. M. Sotomayor-Torres, P. S. Kop'ev, and V. M. Ustinov, Appl. Phys. Lett. **64**, 1526 (1994); P. D. Wang, J. L. Merz, N. N. Ledentsov, P. S. Kop'ev, V. M. Ustinov, and C. M. Sotomayor-Torres, Solid State Commun. **100**, 763 (1996); V. Bressler-Hill, A. Lorke, S. Varma, P. M. Petroff, K. Pond, and W. H. Weinberg, Phys. Rev. B **50**, 8479 (1994).
[2] P. M. Petroff and G. Medeiros-Ribeiro, Mater. Res. Bull. **21**, 50 (1996).
[3] M. C. Bartelt, A. K. Schmid, J. W. Evans, and R. Q. Hwang, Phys. Rev. Lett. **81**, 1901 (1998).
[4] T. I. Kamins and R. S. Williams, Appl. Phys. Lett. **71**, 1201 (1997); J. R. Heath, R. S. Williams, and J. J. Shiang, J. Phys. Chem. **100**, 3144 (1996); T. T. Ngo, P. M. Petroff, H. Sasaki, and J. L. Merz, Phys. Rev. B **53**, 9618 (1996); A. Hartmann, L. Vescan, C. Dieker, and H. Lüth, J. Appl. Phys. **77**, 1959 (1995); S. Jeppesen, M. S. Miller, D. Hessman, B. Kowalski, I. Maximov, and L. Samuelson, Appl. Phys. Lett. **68**, 2228 (1996).
[5] S. Y. Shiraev, F. Jensen, J. L. Hansen, J. W. Petersen, and A. N. Larsen, Phys. Rev. Lett. **78**, 503 (1997).
[6] R. Leon, T. J. Senden, Y. Kim, C. Jagadish, and A. Clark, Phys. Rev. Lett. **78**, 4942 (1997).
[7] D. M. Eigler and E. K. Schweizer, Nature (London) **344**, 524 (1990).
[8] K. Terashima, M. Kondoh, and T. Yoshida, J. Vac. Sci. Technol. A **8**, 581 (1990); S. Yamada and M. Yamamoto, J. Appl. Phys. **79**, 8391 (1996); H. J. Mamin, P. H. Guethner, and D. Rugar, Phys. Rev. Lett. **65**, 2418 (1990).
[9] H. J. Mamin, P. H. Guethner, and D. Rugar, Phys. Rev. Lett. **65**, 2418 (1990).
[10] C. Priester and M. Lannoo, Phys. Rev. Lett. **75**, 93 (1995).
[11] I. Daruka and A.-L. Barabási, Phys. Rev. Lett. **78**, 3027 (1997).
[12] A.-L. Barabási, Appl. Phys. Lett. **70**, 2565 (1997).
[13] A.-L. Barabási and H. E. Stanley, *Fractal Concepts in Surface Growth* (Cambridge University Press, Cambridge, 1995).
[14] S. V. Ghaisas and S. Das Sarma, Phys. Rev. B **46**, 7308 (1992); C. Ratsch, A. Zangwill, P. Smilauer, and D. D. Vvedensky, Phys. Rev. Lett. **72**, 3194 (1994); E. Kaxiras, D. Kandel, Appl. Surf. Sci. **102**, 3 (1996); J. G. Amar, F. Family, and P.-M. Lam, Phys. Rev. B **50**, 8781 (1994).
[15] Since $l_d \sim (D/F)^{\psi_d}$, when D is the diffusion constant of the adatoms, given $D(T) = D_0 \exp(-E_0/kT)$, l_d depends on T as well. Consequently, keeping F constant, the temperature can be used equally efficiently to locate the optimal growth conditions.